A numerical, theoretical and experimental study of the effect of thermocycling on the matrix-filler interface of dental restorative materials

Yoan Boussès, Nathalie Brulat-Bouchard, Pierre-Olivier Bouchard, Yannick Tillier

Version of Record: https://www.sciencedirect.com/science/article/pii/S0109564121000300
Manuscript_d803234ea908a897e26bd51a3c0175d9

A numerical, theoretical and experimental study of the effect of thermocycling on the matrix-filler interface of dental restorative materials

Yoan Boussès[a*], *Nathalie Brulat-Bouchard*[a,b], *Pierre-Olivier Bouchard*[a], *Yannick Tillier*[a]
[a] CEMEF Centre de Mise En Forme des Matériaux, MINES ParisTech, PSL Research University, UMR CNRS 7635, Sophia Antipolis, CS10 207, France
[b] *UFR d'Odontologie Nice Côte d'Azur, Université Nice Sophia Antipolis, Nice, France*
* *corresponding author : yoan.bousses@mines-paristech.fr*

Acknowledgements

This work was supported by the project TOOTHBOX ANR 16-CE08-0024 of the French National Research Agency (ANR). The LMI laboratory is also acknowledged for the exchanges we had. Finally, DMG© is acknowledged for the preparation of the composites and their availability.

1) Introduction

Polymer resin composites are widely used in the restoration of dental decays. In an oral environment, they are facing an aggressive environment. Mechanically, mastication produces complex loads on restorations. Other phenomena such as bruxism cause significant wear to the composites. Chemically, saliva creates an aqueous medium capable of damaging composites. As polar molecules, dental polymers are likely to absorb water. Moreover, the presence of ions can accelerate the hydrolysis of polymer molecules. Food residues also contribute to the degradation of restorations. Last but not least, teeth can face sudden temperature variations because of hot and cold food for example. Due to different thermal expansion coefficients between the tooth, the resin and fillers, thermal variations cause stress in a restoration. It is noteworthy not only at the interface between the tooth and the composite, but also at the interface between the matrix and the fillers.

For these reasons, it is important to study the stability of resin composites over time. In particular, a restoration must keep its mechanical properties unchanged. Several strategies exist to simulate the influence of an oral environment. One of them is to focus on thermal variations in an aqueous environment in vitro. The samples are alternatively plunged into “hot” and “cold” liquids. This process is called thermocycling; it does not take into consideration mechanical fatigue or wear phenomena.

Water is frequently used, but some experiments are done with alcohol or artificial saliva, that is water to which specific ions were added [1]. Moreover, a high diversity of experimental conditions are used because ISO 4049 for polymer-based restorative materials does not impose any standard protocol [2]. From 1970 to 1998, Gale did a review of thermal cycling procedures for laboratory testing of dental restorations [3]. This work was continued by Morresi from 1999 to 2014 [4]. Systematically, low and high temperatures were recorded, as well as dwell times, transfer times and numbers of cycles. There seems to be a consensus for bath temperatures of 5°C and 55°C, especially in recent studies. Indeed, these two extreme temperature values correspond to the pain thresholds of the human body [5]. Such an extreme variation can correspond to the alternating consumption of coffee and ice cream for example. Therefore it is assumed that food with temperatures above or below these threshold values will not be kept in mouth.

The other parameters are more subjected to variations. Number of cycles varied from 100 to 100 000 cycles. However a median value of 500 cycles was found by Gale. The author also suggested that 10 000 cycles correspond to one year of clinical function. This hypothesis assumes that 20 to 50 thermal cycles occur in one day. This equivalence seems to be shared by many authors, but is also disputed. Dwell times are very different too. Some authors considered that such temperatures could not be tolerated for more than a few seconds [6] whereas some numerical simulations suggested that close to one minute of immersion is necessary to homogenize the temperature at the centre of the samples. Dale reported a range from 4 s to 20 min, with a median value of 30 s for dwell time. Regarding the transfer time, ISO 11405 for testing of adhesion to tooth structure [2] recommends between 5 and 10 s. However, the information was not systematically mentioned by the authors. In fact, most parameters seem to be chosen on the basis of convenience without any real justification for the choices made.

With such varied protocols and composites tested, results are very scattered. Some authors found a drastic drop in properties for short artificial aging periods [7, 8], whereas others observed a plateau before a more or less progressive decrease of properties [7, 1, 8, 9]. Some authors never found any decrease [7], or their studies even show an improvement of some properties for a short number of cycles, before a degradation of mechanical properties [10]. This wide range of results may be a consequence of many phenomena that can occur, not all of which are well known. For example, Carreira [10] mentioned that his results were contrary to other studies on the same material with similar ageing conditions. Degradation mechanisms are complex and affect differently the matrix, the fillers and the interface between them [7, 11, 4, 10, 1]. Inorganic fillers are little affected, if ever [11, 4].

Otherwise, the Turcsányi model [12] can help to compare the matrix degradation to that of the interface. Indeed, this model links the yield stress of the composite to that of its matrix, to the filler ratio and to a numerical parameter which is directly correlated to the quality of the interface. This model was initially developed for non-dental materials using tensile test, but was found to be applicable to the 3-point bending test applied to dental materials [13]. This paper aims at showing how

the use of the Turcsányi model enables to compare the evolution of matrix ageing on the one hand, and the interface ageing on the other hand.

For this purpose, yield stress measurements were performed on different composite batches. Each sample is composed of the same matrix and fillers, and was cured with an identical protocol. Each batch includes eight different filler ratios in order to estimate the parameter of Turcsányi's model. Then four batches with different thermocycling protocols were compared. Samples were observed using SEM and a profilometer was used to complete the analysis.

2) Materials and Methods

2.1) Materials

The composite resin, unfilled resin and fillers were supplied by DMG Chemisch-PharmazeutischeFabrik (*Hamburg, Germany*). Bis-GMA is the main component of the matrix (40.3% of the total weight). Triethylene glycol dimethacrylate (TEGDMA, 19.9wt%), urethane dimethacrylate (UDMA, 19.9 wt%) and ethoxylated bisphenol A dimethacrylate (EBPADMA, 19.9 wt%) are also used. Photoinitiators (camphorquinone, 2,4,6-Trimethylbenzodiphenylphosphine oxide) and stabilizers are also embedded in the matrix. Most of the fillers are random-shape silanated barium glass particles (98.6 wt% of the fillers) with an average particle size of 7 µm. This size is larger than what is commonly found in commercial composites, but it allows filler particle tracking and makes microscopic observations easier. Pyrogenic silica particles with an average particle size of 0.04 µm are also used (1.4 wt%).

Eight materials were prepared by DMG© from the matrix and fillers described above, with different filler weight fractions: 0 wt% (no filler), 20 wt%, 30 wt%, 40 wt%, 50 wt%, 60 wt%, 70 wt% and 80 wt%. Thereafter, they will be named DMG0, DMG20, DMG30, DMG40, DMG50, DMG60, DMG70 and DMG80, respectively. They correspond to 0 vol%, 9 vol%, 14 vol%, 21 vol%, 28 vol%, 37 vol%, 48 vol% and 61 vol% filler volume fractions, respectively. The uncured resins were stored between 4 °C and 6 °C without exposure to light.

2.2) Sample preparation

The samples were prepared according to the same protocol that was detailed in a previous study [13]. Bars of 25x2x2 mm^3 were manufactured in a Teflon mould. The light-curing was performed with a curing lamp (*DeepCureParadigm^{MC}, 3M ESPE, Saint-Paul, USA*) whose wavelength was between 430 and 480 nm and whose intensity was 1 470 mW/cm². The resin was separated from the lamp by a mylar sheet and a glass slide. The samples were exposed to the light through five 1cm-diameter holes that overlap by 5 mm. The resin was exposed for 20 s through each hole, starting with the centre of the sample. Then the same sequence was used to expose the samples from the bottom too. Finally, the samples were stored for 24 h in distilled water at 37 °C to complete polymerization. The water was then cooled down to a controlled room temperature for approximately 20 minutes before performing bending tests or thermocycling. Five samples were taken for each thermocycling duration and each filler ratio, for a total of 160 samples.

2.3) Thermocycling

Since there is no standard protocol for thermocycling, our conditions were chosen based on those most commonly used in other studies. Samples were alternatively immersed in water at 5°C and 55°C. They were trapped in a metallic grid to keep them under the water surface. The dwell time was 21 s and the transfer time was 9 s. However, some water still surrounded the samples during the transfer. Therefore this whole process may be equivalent to a 30 seconds immersion in one bath immediately followed by another 30 seconds immersion in the other bath. Motors ensured the continuous movement of water in the tanks (Figure 1). The temperature was controlled with an accuracy of 0.1°C.

Figure 1: Picture of the thermocycling machine

Four series of samples with different thermocycling durations were tested. The numbers of cycles were 0 (no thermocycling), 1 000, 5 000 and 10 000 cycles. Thereafter, these durations are referred as T0, T1, T5 and T10, respectively. At the end of the thermocycling process, samples were stored for 40 minutes at room temperature before the bending test.

It is noteworthy that the campaign lasted for several months. In order to limit the variations that could occur in material properties or experimental conditions during such a long period of time [13], additional reference samples were produced for T5 and T10 batches for each filler ratio. These samples were tested without any previous thermocycling, and the properties were compared to the ones of thermocycled samples. The relative variation directly induced by thermocycling was calculated. Where appropriate, it was used to adjust T5- and T10-properties with respect to batch T0, so as not to bias the analysis by potential phenomena other than thermocycling, such as an ageing of the uncured resin for example.

2.4) Bending test

A ZwickRoellProLinestatic machine (*BZ 2,5/TH1S, Ulm, Germany*) was used to perform the 3-point bending tests according to the recommendations of ISO 4049 [2] (*Figure 2*). The flexural load was imposed by a cylindrical rod with a cross-head speed of 0.75 mm/min. The sample was supported by two other cylindrical rods, which were 20 mm apart. The room temperature was 23.5±0.5 °C.

Force and displacement were measured during the test. The maximal stress σ and deformation ε at the centre of the sample, on the surface subjected to tensile stress, were calculated as follows, using the beam theory:

$$\sigma = \frac{3FL}{2bh^2} \quad (1)$$

$$\varepsilon = \frac{6Dh}{L^2} \quad (2)$$

where F is the applied load, L the distance between the two supporting rods, b the width of the sample and h its thickness. D is the maximum deflection of the centre of the beam. From the stress-strain curve, the yield stress of the composite (σ_{yc}) was calculated using the classic 0.2 %-strain criterion. The stress-strain curves presented a linear variation below 30 MPa. This slope corresponds to the elastic behaviour of the material and leads to the calculation of the flexural modulus with the following formula:

$$E = \frac{L^3}{4bh^3}\left(\frac{dF}{dD}\right)_{(el)} \quad (3)$$

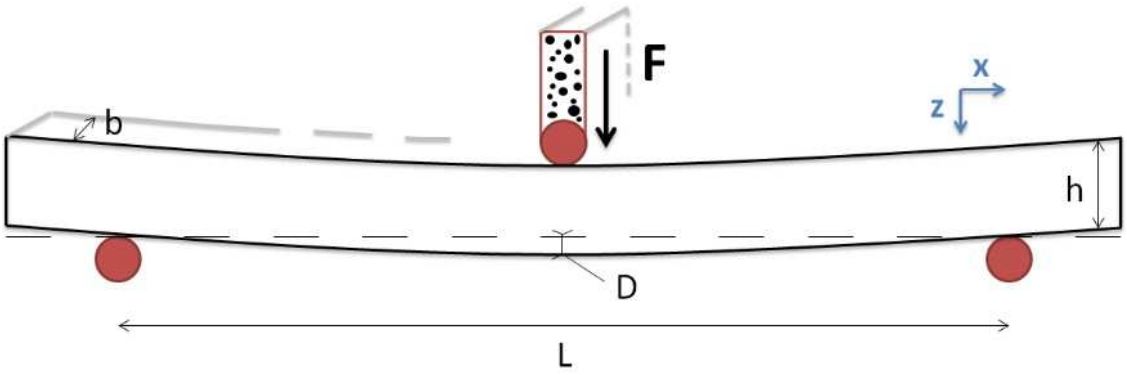

Figure 2 : Drawing of the configuration of the 3-pt bending test

2.5) The Turcsányi and Pukánszky theories

The Turcsányi model [12] enables to predict the yield stress of a composite σ_{yc}, knowing the yield stress of its matrix σ_{y0}, its filler ratio φ, and a numerical parameter related to the quality of the interface between the matrix and the fillers, B. The relation is the following:

$$\frac{\sigma_{yc}}{\sigma_{y0}} = \frac{1-\varphi}{1+2.5\varphi}\exp(B\varphi) \quad (4)$$

This relation was proven to be suitable for dental materials associated to the 3-point bending test [13]. Moreover, Pukánszky [14] managed to express the numerical parameter with respect to some properties of the filler and to the yield stresses of the interface and of the matrix:

$$B = \left(1 + l * A_f * d_f\right) * \ln(\frac{\sigma_{yi}}{\sigma_{y0}}) \quad (5)$$

where l is the interface thickness, A_f is the fillers specific surface area ($m^2.kg^{-1}$), d_f is the filler density ($kg.m^{-3}$) and σ_{yi} is the interface yield stress. In order to calculate σ_{yi}, it was assumed that all the fillers are spherical particles of the same diameter, equal to the average size of the barium glass fillers. Under these conditions, one can write σ_{yi} as:

$$\sigma_{yi} = \sigma_{y0} * exp\left(\frac{B}{1+3*\frac{l}{r}}\right) \quad (6)$$

where r is the mean radius of the particles. This approach underestimates the specific surface area as the particles are not perfectly spherical and because the distribution of particle sizes is not known. The interface thickness could not be measured accurately either. A thickness of 500 nm was estimated from AFM pictures from Ilies's work. With this methodology, the exact value of σ_{yi} is not targeted and is not worth of interest. Nevertheless, a relative comparison is still valid. Therefore getting numerical values for σ_{yi} enables us to understand how the interface and the matrix relatively evolved with different thermocycling durations.

2.6) Surface observations

After the bending tests, the roughness of the fractured surface areas was measured with an optical confocal profilometer STIL CCS Prima, (*Chromatic Confocal Sensor, Aix-en-Provence, France*) with the MG140 optical detector. Samples were beforehand metallised. Then a few micrometres spot of white light sweeps across the surface and the intensity of the reflected light is analysed. As each

wavelength has a different focal length, the most intense reflected wavelength gives information on the distance between the spot and the surface. The coupling with the global reflected intensity enables to draw the profile of the surface. The lateral resolution is 1 µm and the vertical resolution is 30 nm. The roughness analysis was made with the Gwyddion software [15].

Samples were also observed with a Philips XL30 (*Semtech Solutions, Billerica, Massachusets, USA*) environmental Scanning Electron Microscope (SEM). There was no need to metallize the samples metallized prior to observations.

2.7) FEM simulations

Some simulations were made on Abaqus CAE (*Dassault Systèmes, Abaqus 6.14, Providence, RI, USA*) in order to help in the understanding of thermocycling. We were particularly interested in the heat transfer within the sample and its mechanical effects during a thermal cycle. This Finite Element Method (FEM) was used to simulate 25x2x2 mm^3 samples in a water environment. The temperature varied instantaneously from room temperature (23 °C) to 5 °C for one minute, and then to 55 °C for another one minute. A convective heat transfer was used to simulate the interaction between the lateral faces of the sample and its environment, characterized by the heat transfer coefficient $h = 100\ W/m^2$ [10].

A coupled temperature/displacement analysis was performed. A sensitivity study was made to adjust time step and mesh size prior to the complete simulations. The mesh was based on isotropic hexaedral elements, fully integrated and linear (C3D8T element type). The non-linear geometrics option was activated. Three symmetry planes were used to avoid any rigid body motion. Different simulations were carried out with different materials and boundary conditions. They will be detailed further. The parameters used to describe the matrix and the fillers were found in the literature [10] or measured directly on our composite materials. They are presented in Table 1. Fillers were considered as purely elastic whereas the matrix behaviour was visco-elastic with two Prony branches.

Parameter	Matrix	Fillers
Thermal expansion coefficient (K^{-1})	80x 10^{-6}	5x 10^{-6}
Heat capacity at constant pressure ($J.kg^{-1}.K^{-1}$)	1 000	720

Heat transfer coefficient with water ($W.m^{-2}$)	100	100
Thermal conductivity ($W \cdot m^{-1} \cdot K^{-1}$)	0.2	2
Density (kg/dm^3)	1.15	2.5
Elastic modulus (long-term) (GPa)	0.882	70
Poisson's ratio	0.33	0.33

Table 1: Numerical parameters used to simulate thermal cycles in Abaqus for both components of the composite

3) Results

3.1) Temperature evolution in a sample during thermocycling (FEM analysis)

A first preliminary numerical study was carried out to validate the minimal duration of the thermal cycle. A simplified composite (Figure 3) was used to record the evolution of temperature and stresses at the centres of the matrix and filler phases. Except the three symmetry planes that prevent any rigid body motion, no mechanical boundary condition was applied. The results are plotted in Figure 4.

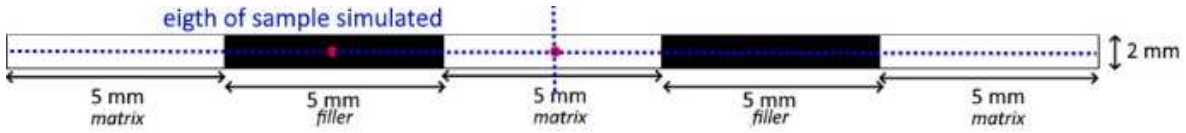

Figure 3: 2D representation of the simplified composite and its symmetry planes, used to record temperature and stress evolutions on the two red spots with Abaqus

As expected, the bulk temperature of the material does not vary as instantaneously as the environment. Nevertheless, the temperature still evolves rapidly and similarly in both phases. Moreover, the internal stress appears to be highly correlated with the temperature as it follows the same trend. Most of the variation occurs within the first 20 seconds of a bath. 30 seconds after a temperature jump of 50 °C, the remaining variations can be considered negligible. During the last 30 seconds of the calculation, the minor temperature changes (and thus the strain and stress) in the sample seem to indicate that it is not relevant to extend the bath beyond half a minute. Moreover, the temperature distribution in the sample (Figure 5) shows that the temperature at the centre of the sample, which is plotted on Figure 4, evolves less rapidly than the average temperature of the whole sample. Thus the average temperature after a 30 s immersion is even closer to the target-temperature than the curves of Figure 4. These results confirm that the 30"/30"-hot/cold thermocycling conditions

we have imposed (section 2.3) are realistic and allow the target temperature values to be reached. This has the advantage of reducing the time of experimental trials without missing important phenomena.

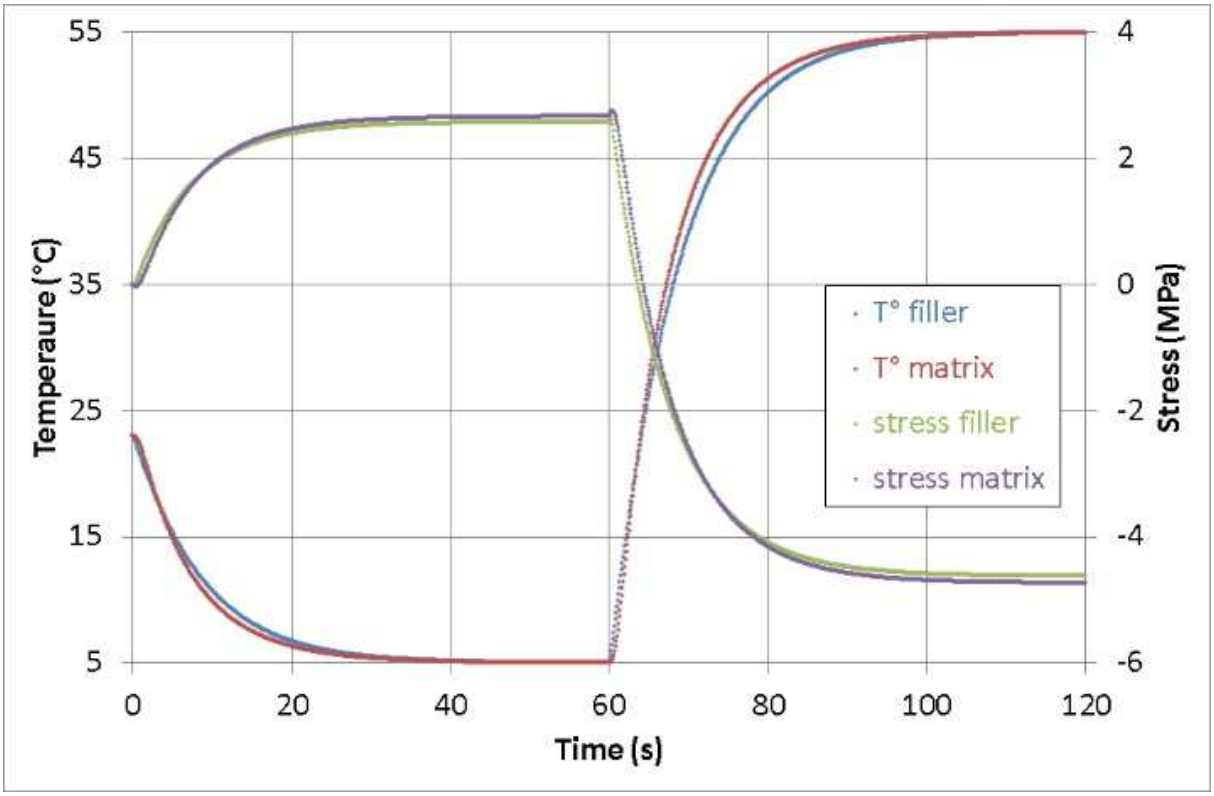

Figure 4: Temperature and stress evolution at the centre of the matrix and the fillers of a composite sample along a thermal cycle

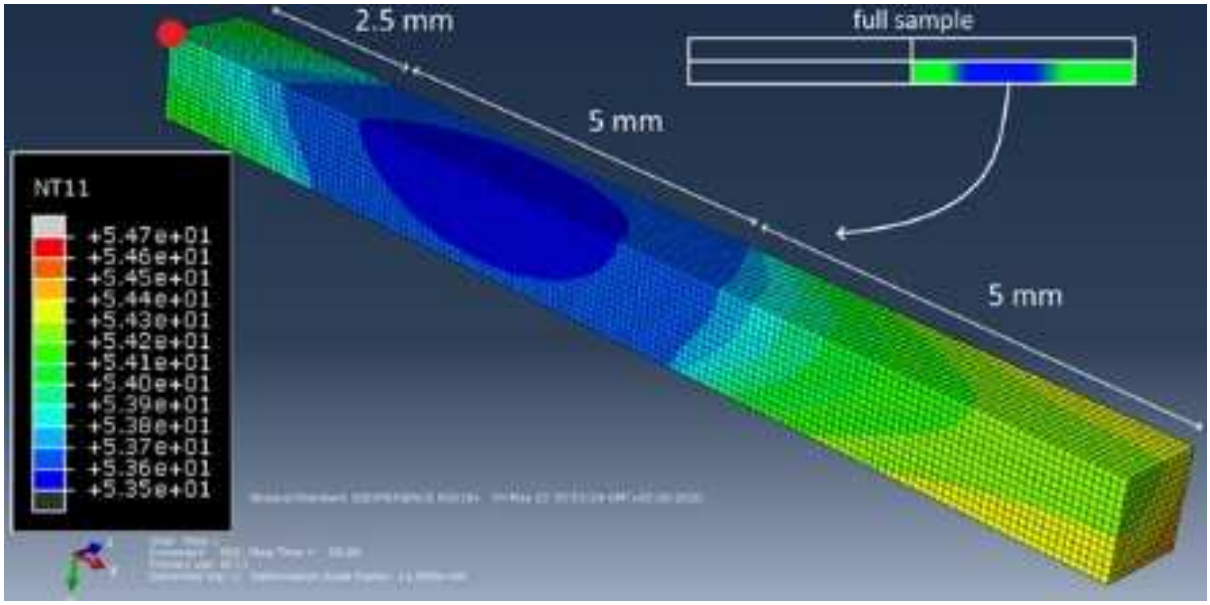

Figure 5: Temperature distribution in an eighth of sample after 90 seconds of cycle. The red spot corresponds to the centre of the entire sample

3.2) Effect of thermocycling on mechanical properties

The measurements of the composite yield stress from the bending tests are summarized in the Table 2. For a given thermocycling duration, the yield stress increases with the filler ratio. For a given filler ratio, increasing thermal cycles leads to yield stress decrease. Some points can be noticed for filler ratios from 40 vol% to 70 vol%, which do not follow the decreasing trend. However, they are marginal and are often combined with a higher standard deviation. The B parameters of the Turcsányi model were also estimated for each thermocycling duration. The four experimental results batches do follow well the model (Figure 6), with determination coefficient (R^2) greater than 0.99 for T0, T1 and T5, and equal to 0.98 for T10. Moreover, even though the yield stress decreased with thermocycling duration, B remains stable at about 4.45 up to 5 000 cycles. It characterizes the ratio between the composite yield stress and the matrix yield stress. This ratio became less important for 10 000 cycles but remains close to 4.45. The interface yield stress was also calculated for each batch. It slightly decreases in the first 5 000 cycles from 1 072 MPa to 1 028 MPa. Then the drop between 5 000 cycles and 10 000 cycles is more important as it falls down to 879 MPa.

		Yield stress (MPa)			
Mass filler ratio	**Volume filler ratio**	**T0**	**T1**	**T5**	**T10**
0 %	0 %	47.82 (3.45)	46.50 (2.00)	44.82 (1.71)	41.80 (1.60)
20 %	9 %	53.53 (2.84)	51.28 (2.04)	50.18 (0.60)	49.35 (1.50)
30 %	14 %	57.46 (4.69)	55.32 (2.11)	51.95 (2.43)	51.77 (1.39)
40 %	21 %	60.08 (2.59)	58.69 (3.57)	61.97 (2.86)	54.51 (1.19)
50 %	28 %	69.54 (1.27)	70.88 (2.62)	65.58 (1.78)	65.78 (1.67)
60 %	37 %	81.24 (4.88)	77.68 (1.04)	79.57 (4.29)	70.05 (2.51)
70 %	48 %	93.12 (2.28)	91.52 (3.88)	92.78 (5.42)	80.20 (0.89)
80 %	61 %	113.54 (4.64)	111.79 (2.84)	103.98 (3.45)	88.62 (2.85)
B (Turcsányi's model)		4.44	4.46	4.47	4.35
Determination coefficient R^2		0.995	0.994	0.991	0.981
σ_{yi} (MPa)		1 072	1 057	1 028	879

Table 2 : Yield stress of resin composites measured by 3-point bending test with respect to thermocycling duration

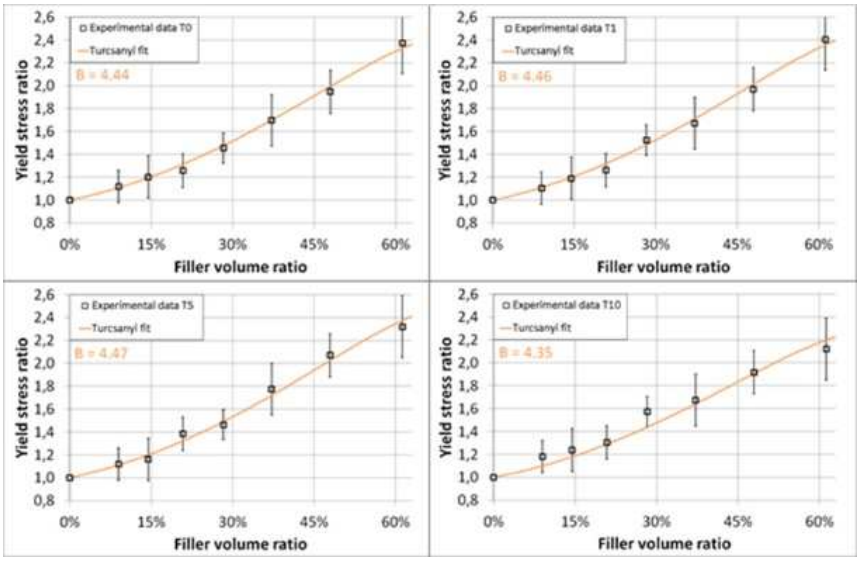

Figure 6: Evolution of composite yield stress with respect to volume filler ratio for each thermocycling duration

The scales of matrix and interface degradation are compared in Table 3. The relative variation of σ_{y0} and σ_{yi} show that the speeds are different. After 1 000 cycles, the yield stress matrix loses 2.8% of its unaged property, whereas the loss is half as great as for the interface. After 5 000 cycles, the yield stress matrix decreased for 6.3% whereas it was only 4.1% for the interface. After 10 000 cycles, the matrix loss continued to follow a linear trend to reach 12.6%. On the contrary, the interface yield stress suffered a sudden loss, dropping from -4.1% to -18.0%. Therefore, for the longest thermocycling process, the interface appeared to be more damaged than the matrix.

	T0	**T1**	**T5**	**T10**
Relative variation σ_{y0}	-	-2.8%	-6.3%	-12.6%
Relative variation σ_{yi}	-	-1.4%	-4.1%	-18.0%

Table 3: Comparison of the evolution of σ_{y0} and σ_{yi} with respect to the number of thermal cycles

The flexural modulus results followed a similar trend. The effect of thermocycling is visible too on the (absolute) properties of Table 4; they decrease as the number of thermal cycles increase. The flexural modulus ratios are also compared. Figure 7 presents the evolution of the composite modulus relatively to the matrix modulus with respect to the filler ratio. The curves for T0, T1 and T5 are very similar, whereas the T10-curve stands out with a slower increase. This evolution is similar to the yield stress plots. Nevertheless, no accurate theoretical model linking flexural modulus and interface quality was found for high filler ratio, such as the Turcsányi model for the yield stress [13]. Thus it is not

possible to correlate these curves to an evolution of the interface quality. Graphically, the same observation as for the yield stress is made: the curves for T0, T1 and T5 are very similar, whereas the T10-curve stands out with a slower increase.

		Flexural modulus (GPa)			
Mass filler ratio	**Volume filler ratio**	**T0**	**T1**	**T5**	**T10**
0 %	0 %	1.51 (0.07)	1.45 (0.05)	1.43 (0.05)	1.30 (0.03)
20 %	9 %	2.09 (0.08)	2.04 (0.10)	1.82 (0.06)	1.88 (0.07)
30 %	14 %	2.36 (0.08)	2.29 (0.15)	2.25 (0.12)	2.15 (0.13)
40 %	21 %	2.87 (0.13)	2.96 (0.21)	2.76 (0.16)	2.50 (0.07)
50 %	28 %	3.80 (0.16)	3.88 (0.25)	3.74 (0.13)	3.57 (0.10)
60 %	37 %	4.85 (0.26)	4.87 (0.05)	4.77 (0.35)	4.11 (0.11)
70 %	48 %	6.68 (0.37)	6.63 (0.33)	6.58 (0.31)	5.99 (0.34)
80 %	61 %	9.90 (0.37)	10.24 (0.44)	9.09 (0.58)	8.01 (0.10)

Table 4: Flexural modulus of resin composites measured by 3-point bending test with respect to thermocycling duration

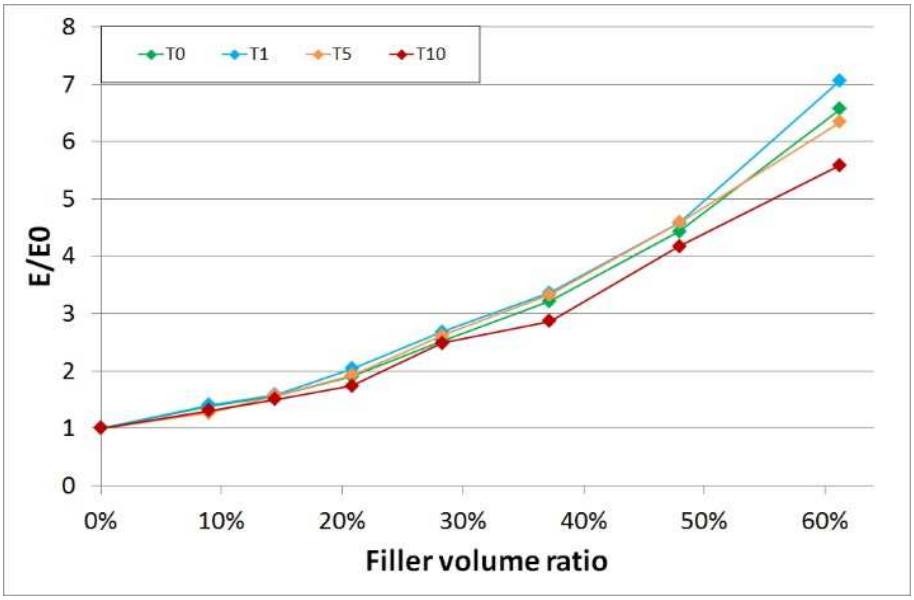

Figure 7: Evolution of the flexural modulus ratio with respect to the filler volume ratio for different thermocycling durations

3.3) Profilometry measurements

The fracture surface roughness of several samples from different filler ratios and thermocycling durations was measured. The results are reported in Table 5. The roughness was between 4 and 10 µm but no evolution could be measured with respect to the number of thermal cycles or the filler ratio. However, these results were obtained after removing the points with no signal. These amounts of removed points were not quantifiable but the difference between unaged and thermocycled samples

was qualitatively obvious. Figure 8 shows the example of three pictures (with same scale) of DMG70-samples that were exposed to 0, 5 000 and 10 000 thermal cycles, respectively. The unaged sample showed few disconnected points whereas they were very numerous for the T10 sample. The T5 sample had slightly more disconnected points than the T0 sample but was far from the T10 state. The same comparison was made for every filler ratio, except for the unfilled sample, whose surfaces were smooth.

Roughness (Ra) (µm)	T0	T5	T10
DMG 0		*	
DMG 30	4.946	4.254	7.761
DMG 50	10.369	6.394	8.003
DMG 70	8.055	7.05	6.947
DMG 80	6.905	9.058	*

*Table 5: Fracture surface Ra roughness of samples from different protocol conditions. * means that the roughness was not measurable on these samples.*

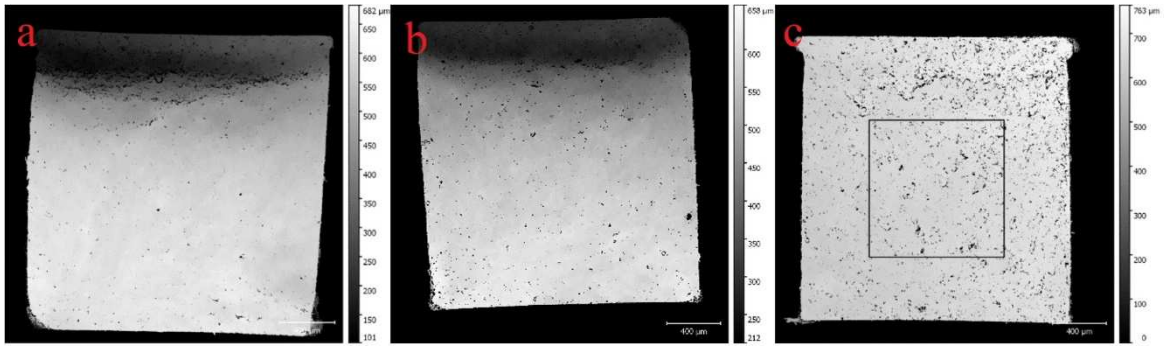

Figure 8 : « Altitude » signal given by Gwyddion software from profilometer data for three DMG70 samples thermocycled during 0 (a), 5 000 (b) and 10 000 cycles (c). Black points correspond to a signal loss. The square on picture c shows the area where the roughness were calculated to avoid any bias from the edges of the samples.

3.4) Samples failure and SEM observations

SEM observations of the fracture areas were made to get a better understanding of composite ageing. Figure 9 compares the fracture area of two DMG40 composites, respectively unaged and thermocycled for 10 000 cycles. Both pictures show a rough surface with some apparent fillers and matrix deformation. One can estimate that the T10 sample is rougher with more apparent particles. However, contrary to the profilometer images, it is difficult to quantify a real difference between the two failure surfaces with the SEM.

For different ageing conditions and filler ratios, the two fracture surfaces from the same broken sample were also observed in a mirror layout. Zooms on the pictures shown on Figure 7 and on their opposite faces are presented on Figure 10 and Figure 11. Several phenomena are highlighted. In the red circle, a filler is neatly broken into two parts. There is no relief around it and the fracture surface is planar; the crack propagated in a straight line. This configuration is frequent and can be observed on other spots of the picture. In the blue circle, it looks like the result of a debonding. The "hole" on the one side matches well with the pulled off particle on the opposite side. However, it is only partially uncovered, the matrix remaining partly stuck to at least half of the particle surface. A more extreme case is highlighted by the green circle. There, the shape of a particle is visible but it is completely covered by matrix. The complementary ridges on each side, which cannot appear on glass, are proof of this. Finally, on the purple circle, a broken particle is highlighted.

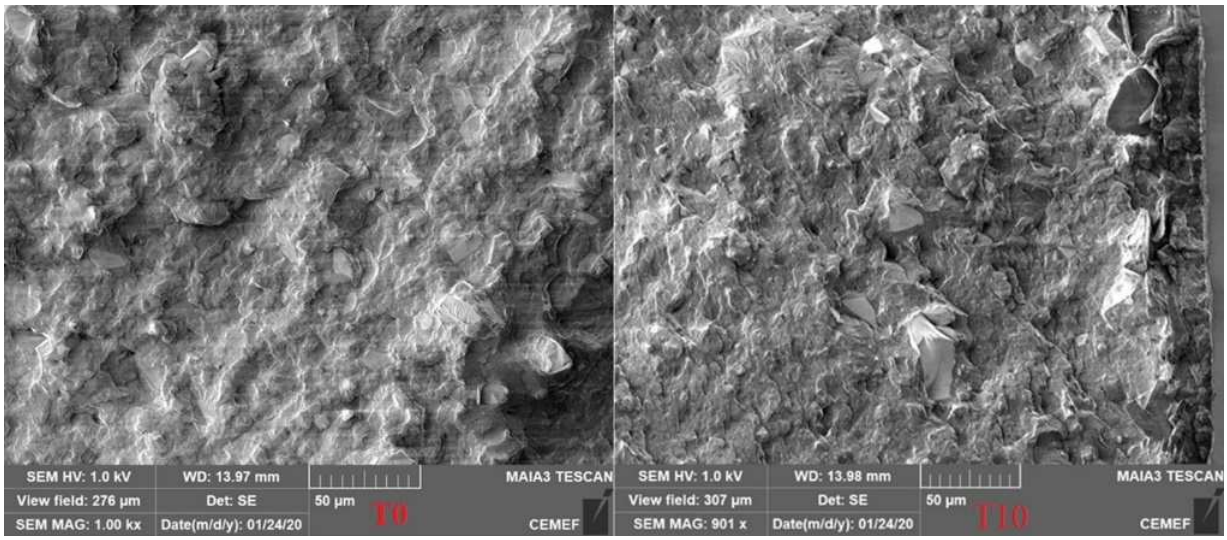

Figure 9: SEM pictures of the fracture area of a DMG40 composite after 0 (T0, left) and 10 000 (T10, right) thermal cycles

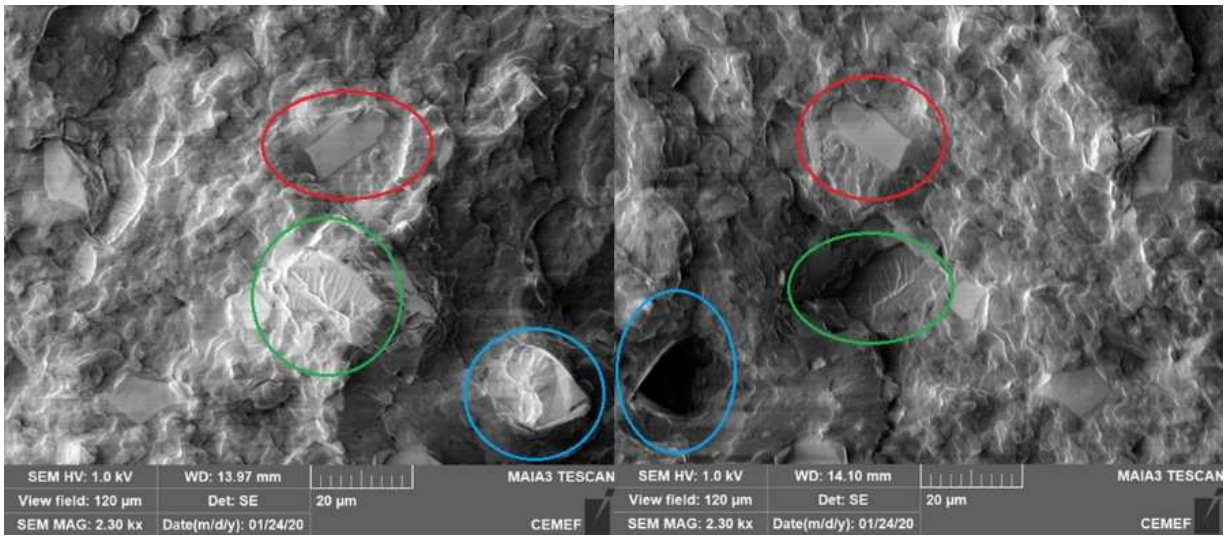

Figure 10: SEM pictures of unaged 40 wt% composite on two opposite sides of the fracture area (mirror layout)

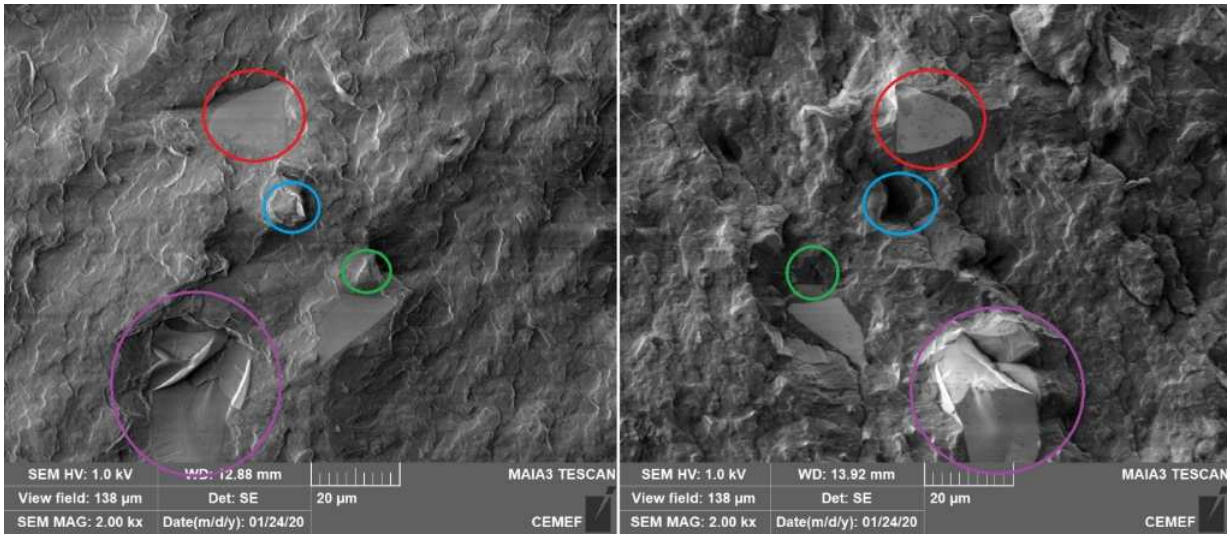

Figure 11: SEM pictures of a 40 wt% composite after 10 cycles on two opposite sides of the fracture area (mirror layout)

3.5) Stress and strain distribution along the sample (FEM analysis)

Temperature changes induce volume variations of a free material. However, in a tooth, a composite has to adapt to adapt to boundary conditions that limit its movements. It leads to internal thermal stress. FE simulations can help to understand how this stress is distributed in the composite.

For this purpose, further FE simulations were performed on two samples. One is a full-matrix sample and the other is the composite sample presented in Figure 3. The same thermal cycle was applied but, this time, the sample was fixed at its extremities to represent the boundary conditions of a restoration. After a thermal cycle of 120s, stress and mechanical strain were plotted along the sample.

The values for the matrix areas in both samples were compared. This comparison is thus only valid in the ranges [0;5mm], [10;15mm] and [20;25mm] on Figure 12, where there is matrix in both configuration. In the ranges [5;10mm] and [15;20mm], the material can be matrix or filler, depending on the simulation. Therefore the comparison makes no sense in these two ranges, and there are logically great differences in stress and strain.

For a full-matrix sample, strain and stress become constant 3 mm beyond its extremities. For a composite configuration, the evolution is more complex. The matrix length between the fillers (5 mm) is therefore not long enough to reach a plateau. This explains that the stress is not constant along the matrix areas. In both configurations, there are peaks of stress and strain less than 1 mm to the interface. They are higher for the composite sample than for the sample fully made of matrix. The mean stress and strain values are also higher in the matrix area of the composite than in the full-matrix sample.

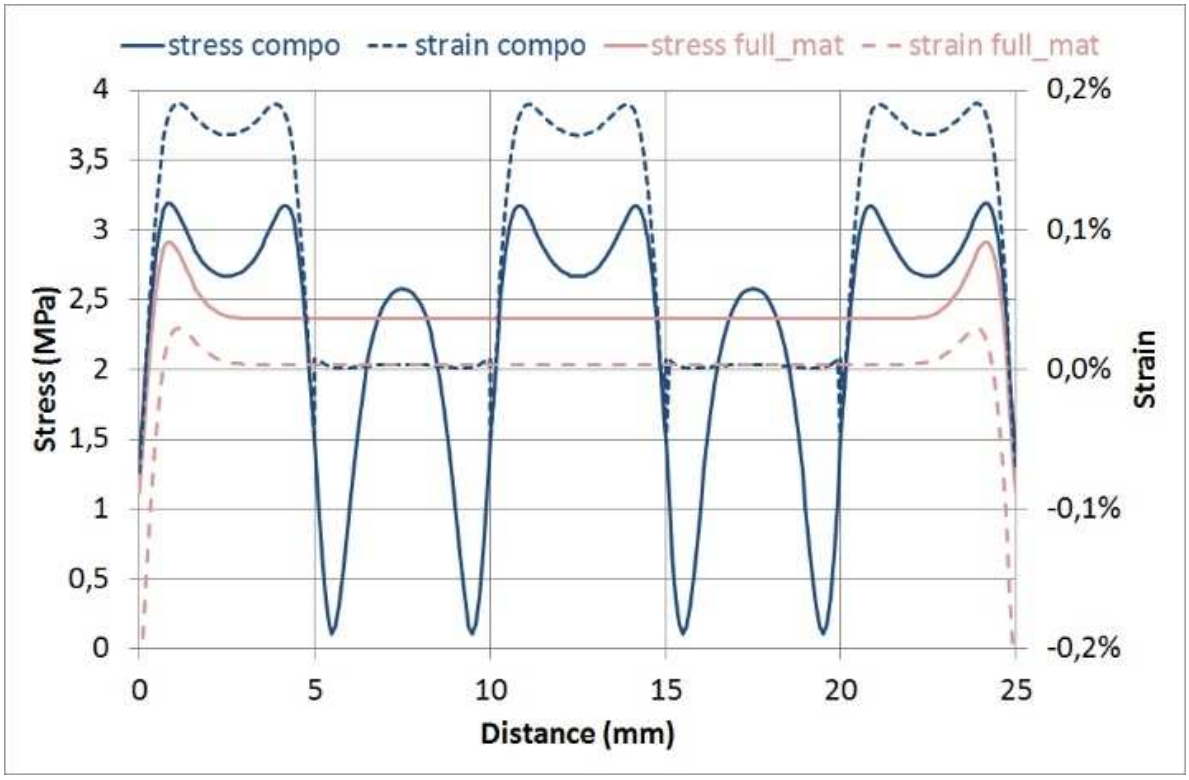

Figure 12: FEM evolution of stress and mechanical strain along the sample for a composite sample and a full-matrix sample immediately after a full thermal cycle of 120 s. The composite configuration of the first simulation is reminded below the graph

4) Discussion

The preliminary numerical study (Figure 4) showed that a 30 s-immersion of a 25x2x2 mm^3-sample in water is enough to homogenise the temperature within a sample. In particular, the temperature at the centre of the sample is nearly equal to the one at the surface. Temperature variations in the immersion times were a point raised by Gale and Morresi reviews [3,4]. Here, it seems that (30"/30")-cycles are sufficient to reach the extreme temperatures of 5°C and 55°C. These temperatures are directly correlated to the stress in the composite. Such a short cycle duration time could eventually underestimate some viscous effects in the medium term, but this phenomenon is not likely to occur in the mouth a priori. The positive effect is to reduce efficiently the time of experimental campaigns.

The experimental study showed that thermocycling does have an impact on the composite properties. On a macroscopic scale, the good preservation of the properties observed for the first 1 000 cycles is comparable to the evolution of Carreira's results [10], who also found that the main properties (flexural strength, Work Of Fracture, micro-hardness) remain stable after 1 500 cycles between 5°C and 55°C. Considering the equivalence between 10 000 cycles and one year *in-vivo* of the restoration, 1 000 cycles correspond to less than two months; it seems rather reassuring that resin composites do not lose their properties after such a short time. Nevertheless, it is quite difficult to compare our results to those of other studies because, as reported in Gale and Morresi reviews [3,4], distinct laboratories can obtain very different results despite using apparent same protocols.

Regarding our study, yield stress and flexural modulus underwent a similar decrease of their properties. After 1 000 cycles, the loss is between 0% and 4%. Some batches even show a slight increase of their values, for example DMG50, but it does not seem significant since the variation is always in the range of the standard deviations. Composites with the lowest filler ratios had a relative variation closer to 4% whereas the more filled composites had more stable properties between 0 and 1 000 cycles. After 5 000 cycles, the relative variations are between -1% and -8%. The trends are more scattered after thermocycling but, once again, the less filled composites experienced a greater relative loss than more filled composites. After 10 000 cycles, the relative variations are between -9% and -

15%, except for the 80 wt% filled composite whose loss is about -20%. This time, the most filled composites experienced a greater relative loss than the less filled composites. This observation seems to be consistent with the fact that composites age differently depending on their filler ratios.

The Turcsányi (4) and Pukánszky (5) equations that led to the results shown in Table 3 help to understand the origin of this phenomenon. Indeed, the decrease of matrix yield stress is nearly linear over time. On the other hand, the interface yield stress undergoes a sharp drop between 5 000 and 10 000 thermal cycles whereas its decrease was slow before. This means that the interface aged more slowly than the matrix at the beginning of thermocycling, and then more rapidly after 5 000 thermal cycles. As there is less matrix and more interface when the filler ratio increases, this explains why the composite macroscopic relative losses are different for the same thermocycling duration but different filler ratios.

The profilometry measurements illustrate this phenomenon too. It was noticed that disconnected points were much more present after 10 000 cycles than for shorter durations. These black dots in Figure 8 correspond to areas where no reflected signal was received by the sensor of the profilometer. This can occur when no metallisation could be done on this area, when the slope of the surface is too steep, or when multiple reflections against multiple walls cause too massive signal reduction. These three cases correspond to a “hole” at the surface. In our case, these holes are caused by debonded particles which are missing on one surface of the fracture area, as can be seen in Figure 10. It means that the number of debonded particles is much more important after 10 000 cycles. Moreover, a debonding is the consequence of a weakness at or around the interface between the matrix and the particle, as it becomes easier to bypass the particles rather than to crack them. This confirms that the filler-matrix interfaces were relatively spared during the first 5 000 cycles, and that the damage begins afterwards.

From a chemical point of view, composite samples still uptake water during thermocycling. Moreover, the successive contractions and expansions of the material due to temperature variations create fatigue micro-cracks that help water to penetrate into the matrix. These micro-cracks can appear

in the matrix, and especially at the interfaces between the matrix and the fillers because of different thermal expansion coefficients, which generate local overstress close to the interface. This interphase area frequently undergoes local plasticizing or micro-cracks to drastically reduce its energy. It is also well known that siloxane bonds, resulting from the silanization surface treatment of the fillers, offer a very weak resistance to hydrolysis [7, 4]. But at the beginning of thermocycling, the interphases are protected by the matrix and are therefore barely affected. Once water has propagated through the matrix and reaches the interphase, its siloxane bonds and its micro-cracks, the interphase is severely damaged, leading to an accelerated decrease of the interface yield stress. Moreover, Ghavami measured that the Degree of Conversion (DC) of a commercial composite was still increasing in the first 4 000 thermal cycles of his study [16]. As a result, the water firstly absorbed by the composite could be trapped in the matrix to increase its DC, instead of damaging the interface. Thus the decrease of interface properties would be all the more delayed. As the mechanical properties of the matrix are strongly correlated to the DC too, the first thousands of cycles see two competitive phenomena facing up. Between the micro-cracking of the matrix and the increase of its DC, the macroscopic losses of properties are initially slow.

Numerical simulations, though based on simplified composite geometry, help to understand where cracks are likely to initiate. It is noteworthy that our model does not take into account plasticity or damage and fracture phenomena. The matrix behaviour is considered as visco-elastic and the interface as perfect and infinitely thin. Figure 12 represents a full-length sample with unrealistic enormous fillers, but a scaling gives an idea of what could happen at the microscopic level, to the matrix between particles. Indeed, in response to temperature changes, the matrix cannot expand or retract as freely as it would without fillers. Their high elastic modulus and low expansion coefficient make fillers act as immobile anchor points for the matrix, in a similar way to how the boundary conditions have an impact on numerical simulations. Overstrains and overstress occur at distance but still close to the interface. This area is the most likely to undergo micro-cracks after several thermal cycles. Then, water can later rush into these small gaps to enlarge them and enhance the hydrolysis of the interphase near the interface. Moreover, SEM pictures showed that debonded particles are easily spotted but that

a small amount of matrix also remains around them. It seems to confirm that the cracks propagated close to the interface but not directly within it.

In addition, SEM pictures confirmed the conclusions given by the Turcsányi's theory. Indeed, it predicted that the interface quality remained good even after 10 000 cycles (*B* value higher than 4). In Figure 11, some particles were broken (red and purple circles) after that the crack split them instead of bypassing them. This phenomenon can be observed multiple times on every sample. Moreover, even for debonded particles, matrix often remains stuck to them (blue and green circles). It corresponds to a cohesive failure (in opposition to an adhesive failure where the crack propagates directly at the interface). Bascom [17] confirmed years ago that a failure is adhesive if only the interface is not well prepared. Therefore, this is not the case for the composites of this study. Cohesive failures are even more visible for unaged composites, confirming the good quality of the interface treatment shown in a previous study [13].

5) Conclusion

In the present study, the influence of thermocycling on dental composites was evaluated in different ways. FEM simulations showed that immersions of 30 s are sufficient to reach 5°C and 55°C at the centre of the samples. These conditions were used to age composites during 1 000, 5 000 and 10 000 cycles. Yield stress measurements, on which the Turcsányi and Pukánszky theories were applied, showed that the matrix and the interface do not age at the same rate. In the first 5 000 cycles, the matrix acts as a shield which protects the interfaces from fast damage. Between 5 000 and 10 000 cycles, water reaches the interface. This area is very sensitive to water and is quickly damaged, leading to more important debonded particles and macroscopic loss for yield stress and flexural modulus measured from the three-point bending test. However, SEM and profilometer pictures showed that the cracks propagated in the interphase around the fillers and not directly at the interface between the matrix and the fillers.

Acknowledgements

This work was supported by the project TOOTHBOX ANR 16-CE08-0024 of the French National Research Agency (ANR). The LMI laboratory is also acknowledged for the exchanges we had. Finally, DMG© is acknowledged for the preparation of the composites and their availability.

References

[1] Brendeke J, Ozcan M. Effect of physicochemical aging conditions on the composite-composite repair bond strength. J Adhes Dent 2007;9:399–406.

[2] ISO. Dentistry – Polymer-based restorative materials. ISO 4049. 2009. 28p.

[3] Gale MS, Darvell BW. Thermal cycling procedures for laboratory testing of dental restorations. Journal of Dentistry 1999;27:89–99. https://doi.org/10.1016/S0300-5712(98)00037-2.

[4] Morresi AL, D'Amario M, Capogreco M, Gatto R, Marzo G, D'Arcangelo C, et al. Thermal cycling for restorative materials: Does a standardized protocol exist in laboratory testing? A literature review. Journal of the Mechanical Behavior of Biomedical Materials 2014;29:295–308. https://doi.org/10.1016/j.jmbbm.2013.09.013.

[5] Palmer DS, Barco MT, Billy EJ. Temperature extremes produced orally by hot and cold liquids. The Journal of Prosthetic Dentistry 1992;67:325–7. https://doi.org/10.1016/0022-3913(92)90239-7.

[6] Plant CG, Jones DW, Darvell BW. The heat evolved and temperatures attained during setting of restorative materials. Br Dent J 1974;137:233–8. https://doi.org/10.1038/sj.bdj.4803293.

[7] Ilie N, Hickel R. Macro-, micro- and nano-mechanical investigations on silorane and methacrylate-based composites. Dental Materials 2009;25:810–9. https://doi.org/10.1016/j.dental.2009.02.005.

[8] Egilmez F, Ergun G, Cekic-Nagas I, Vallittu PK, Lassila LVJ. Does artificial aging affect mechanical properties of CAD/CAM composite materials. Journal of Prosthodontic Research 2018;62:65–74. https://doi.org/10.1016/j.jpor.2017.06.001.

[9] Ayatollahi MR, Yahya MY, Karimzadeh A, Nikkhooyifar M, Ayob A. Effects of temperature change and beverage on mechanical and tribological properties of dental restorative composites. Materials Science and Engineering: C 2015;54:69–75. https://doi.org/10.1016/j.msec.2015.05.004.

[10] Carreira M, Antunes P, Ramalho A, Paula A, Carrilho E. Thermocycling effect on mechanical and tribological characterization of two indirect dental restorative materials. J Braz Soc Mech Sci & Eng 2017:39:1-17.

[11] Ilie N, Hickel R, Watts DC. Spatial and cure-time distribution of dynamic-mechanical properties of a dimethacrylate nano-composite. Dental Materials 2009;25:411–8. https://doi.org/10.1016/j.dental.2008.11.008.

[12] Turcsányi B, Pukánszky B, Tüdõs F. Composition dependence of tensile yield stress in filled polymers. J Mater Sci Lett 1988;7:160–2. https://doi.org/10.1007/BF01730605.

[13] Boussès Y, Brulat-Bouchard N, Bouchard P-O, Abouelleil H, Tillier Y. Theoretical prediction of dental composites yield stress and flexural modulus based on filler volume ratio. Dental Materials 2020;36:97–107. https://doi.org/10.1016/j.dental.2019.10.012.

[14] Pukánszky B. Influence of interface interaction on the ultimate tensile properties of polymer composites. Composites 1990;21:255–62. https://doi.org/10.1016/0010-4361(90)90240-W.

[15] Nečas D, Klapetek P. Gwyddion: an open-source software for SPM data analysis. Open Physics 2012;10:181–8. https://doi.org/10.2478/s11534-011-0096-2.

[16] Ghavami-Lahiji M, Firouzmanesh M, Bagheri H, Jafarzadeh Kashi TS, Razazpour F, Behroozibakhsh M. The effect of thermocycling on the degree of conversion and mechanical properties of a microhybrid dental resin composite. Restor Dent Endod 2018;43:e26. https://doi.org/10.5395/rde.2018.43.e26.

[17] Bascom WD, Timmons CO, Jones RL. Apparent interfacial failure in mixed-mode adhesive fracture. J Mater Sci 1975;10:1037–48. https://doi.org/10.1007/BF00823223.